Stem Cell Reports, Volume *19*

Supplemental Information

Rod-shaped micropatterning enhances the electrophysiological maturation of cardiomyocytes derived from human induced pluripotent stem cells

Zeina R. Al Sayed, Charlène Jouve, Magali Seguret, Andrea Ruiz-Velasco, Céline Pereira, David-Alexandre Trégouët, and Jean-Sébastien Hulot

Rod-shaped micropatterning enhances the electrophysiological maturation of cardiomyocytes derived from human induced pluripotent stem cells

Running title: Rod-shaped micropatterning of hiPSC-cardiomyocytes

Zeina R. Al Sayed* [a] PhD, Charlène Jouve* [a] MSC, Magali Seguret [a] MS, Andrea Ruiz-Velasco [a] PhD, Céline Pereira [a] MS, David-Alexandre Trégouët [b] PhD, Jean-Sébastien Hulot [a,c] MD PhD

* Both authors contributed equally to this work

[a] Université de Paris Cité, PARCC, INSERM, F-75006 Paris, France.

[b] INSERM UMR_S 1219, Bordeaux Population Health Research Center, University of Bordeaux, France

[c] CIC1418 and DMU CARTE, AP-HP, Hôpital Européen Georges-Pompidou, F-75015, Paris, France.

SUPPLEMENTAL MATERIAL

Supplemental figures: 5

Supplemental Table: 1

Supplemental Movies: 2

Figure S1. characterization of hiPSC and hiPSC-CMs, related to Figure 1

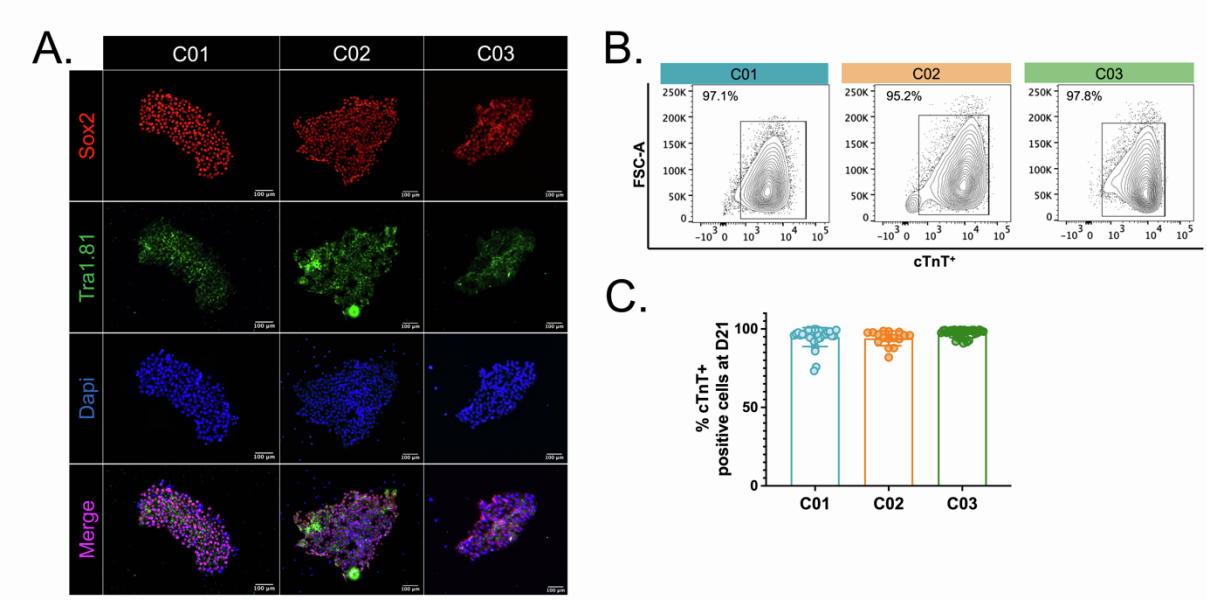

(A) Representative immunofluorescence staining for pluripotency markers for the three hiPSC lines (40X magnification).
(B) Representative flow cytometry plots of D21 hiPSC-CMs showing cTnT-positive cell population for the three hiPSC lines.
(C) Bar graph shows summary of fluorescence-activated cell sorting (FACS) analysis for cTnT+ hiPSC-CMs at day 21 (n = 16-33 differentiations).

Figure S2. Characterization of cells in the individual rod-shaped micropattern, related to Figure 1

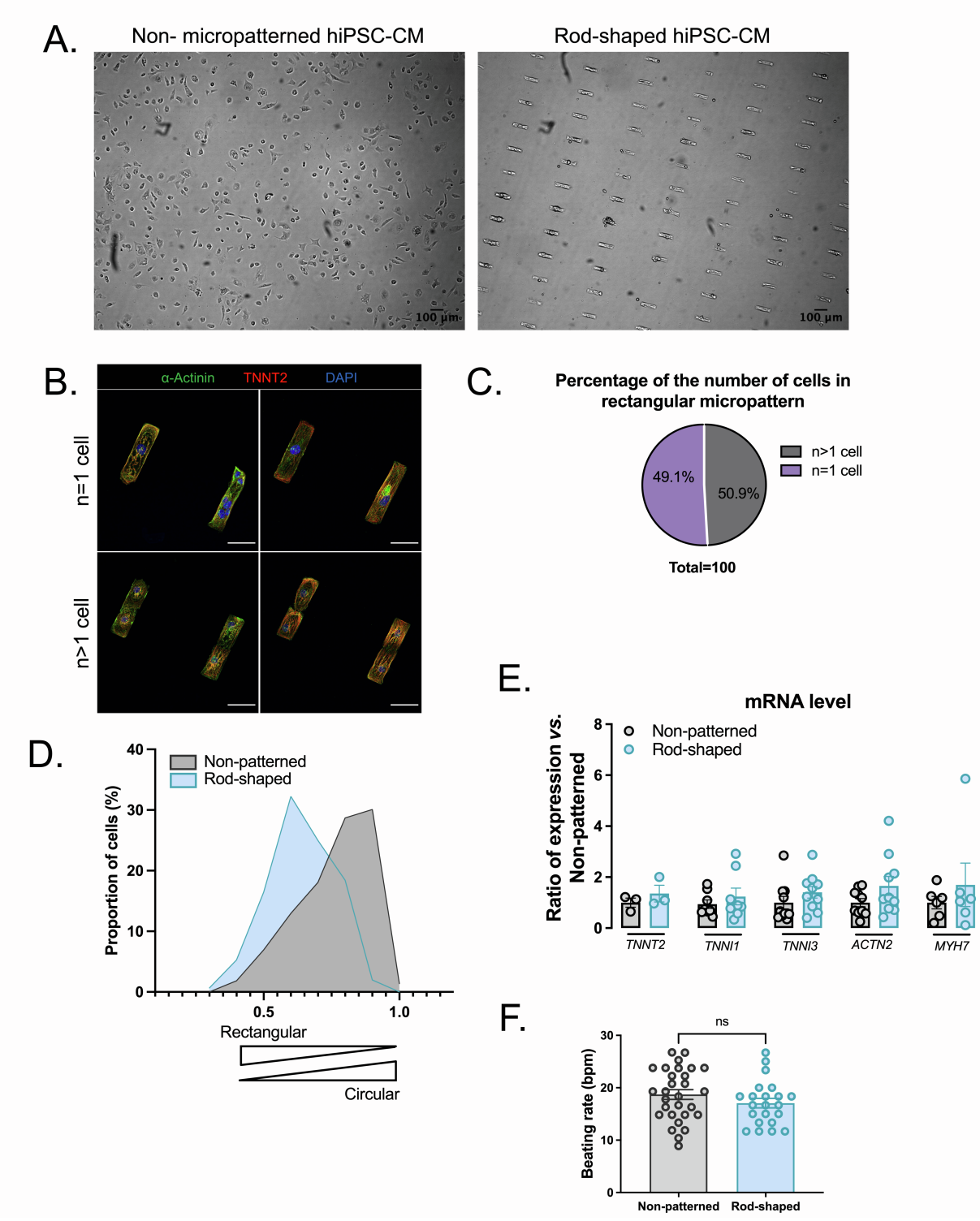

(A) Representative phase-contrast microscopy images of hiPSC-CMs cultured in the non-patterned conditions (left) or on the rod-shaped micropatterns (right)
(B) Representative immunofluorescence images of the number of cells present in individual rectangles in the rod-shaped micropatterns, scale bar = 50 µm
(C) Pie chart showing the distribution of the number of cells in the rod-shaped micropatterns, averaged from the three hiPSC-CMs lines.
(D) Relative distribution of the cell circularity index in both conditions (rod-shaped (n=152 cells) in blue vs. non-patterned (n=216 cells) in grey). An index of 1 corresponds to a circle and of 0.5 to a rectangle.

(E) RNA expression of *TNNT2*, *TNNI1*, *TNNI3, ACTN2* and *MYH7* measured by SYBR green in non-patterned and rod-shaped hiPSC-CMs. Cts were normalized to RPL32 and the ratio rod-shaped *vs.* non-patterned was calculated for each cardiac differentiation.
(F) Spontaneous beating rates measured on videos recordings (rod-shaped (n=22 cells) in blue vs. non-patterned (n=29 cells) in grey).
Data are presented as mean of 3 independent experiments for the three hiPSCs lines. Mann-Whitney: **** $P<0.0001$.

Figure S3. Representative patch clamp experiments in non-patterned and rod-shaped hiPSC-CMs, related to Figures 2-4

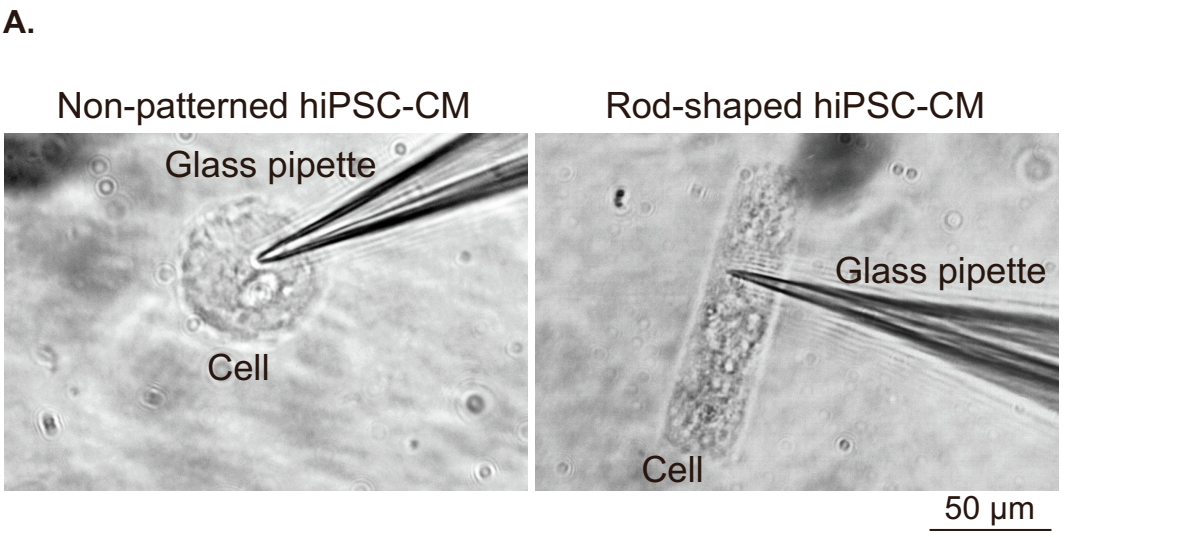

(A) Phase-contrast microscopy images showing a borosilicate patch pipette next to non-patterned (left) and rod-shaped (right) hiPSC-CMs. Images were taken with an X40 objective, scale bar = 50 µm.

(B) Box whisker blot of AP duration (APD) at 30, 50, and 90% repolarization analyzed in non-patterned and rod-shaped hiPSC-CMs paced at 1Hz. Mixed effects analysis with Bonferroni: ns $P>0.05$ *vs.* non-patterned hiPSC-CMs.
(C) Scatter plot of I_{Na} density (pA/pF) in hiPSC-CM for voltage clamp pulse -20 mV from a holding potential -100 mV. The inset shows the voltage protocol.
(D) Scatter plot of averaged cell capacitance (pF).

Data are presented as mean ± SEM. n = 20-28 cells from 4 independent experiments. Mann-Whitney: ns $P>0.05$, and *** $P<0.001$.

Figure S4. Expression of sodium channels subunits, related to Figure 4

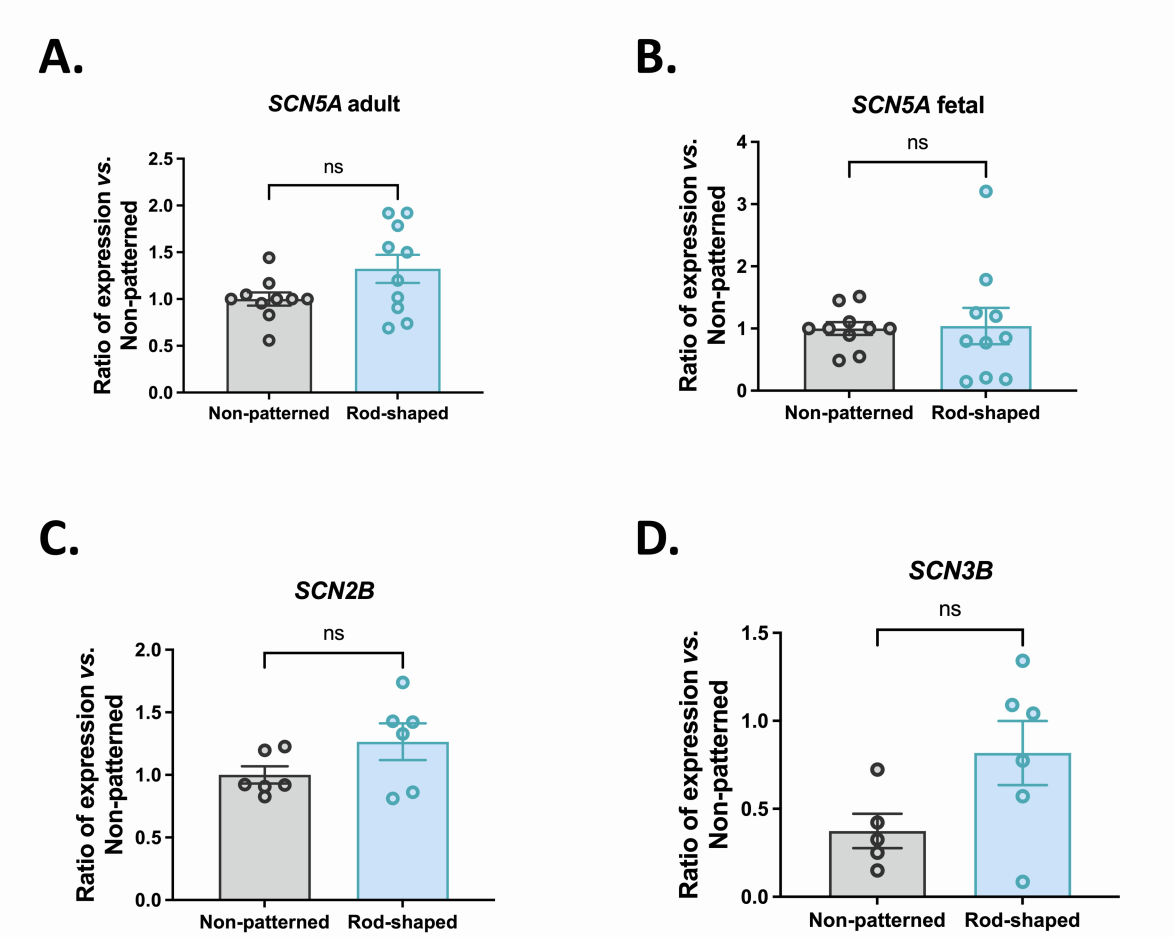

(A-B). RNA expression of adult and fetal *SCN5A* measured by SYBR green in non-patterned and rod-shaped hiPSC-CMs. Cts were normalized to *RPL32*.
(C-D) RNA expression of *SCN2B* and *SCN3B* measured by SYBR green in non-patterned and rod-shaped hiPSC-CMs. Cts were normalized to *RPL32* and the ratio rod-shaped *vs.* non-patterned was calculated for each cardiac differentiation.
n = 3 independent experiments of 5-7 differentiations per condition. Mann-Whitney, ns $P>0.05$.

Figure S5. Calcium handling properties in non-paced non-patterned and rod-shaped hiPSC-CMs, related to Figure 5

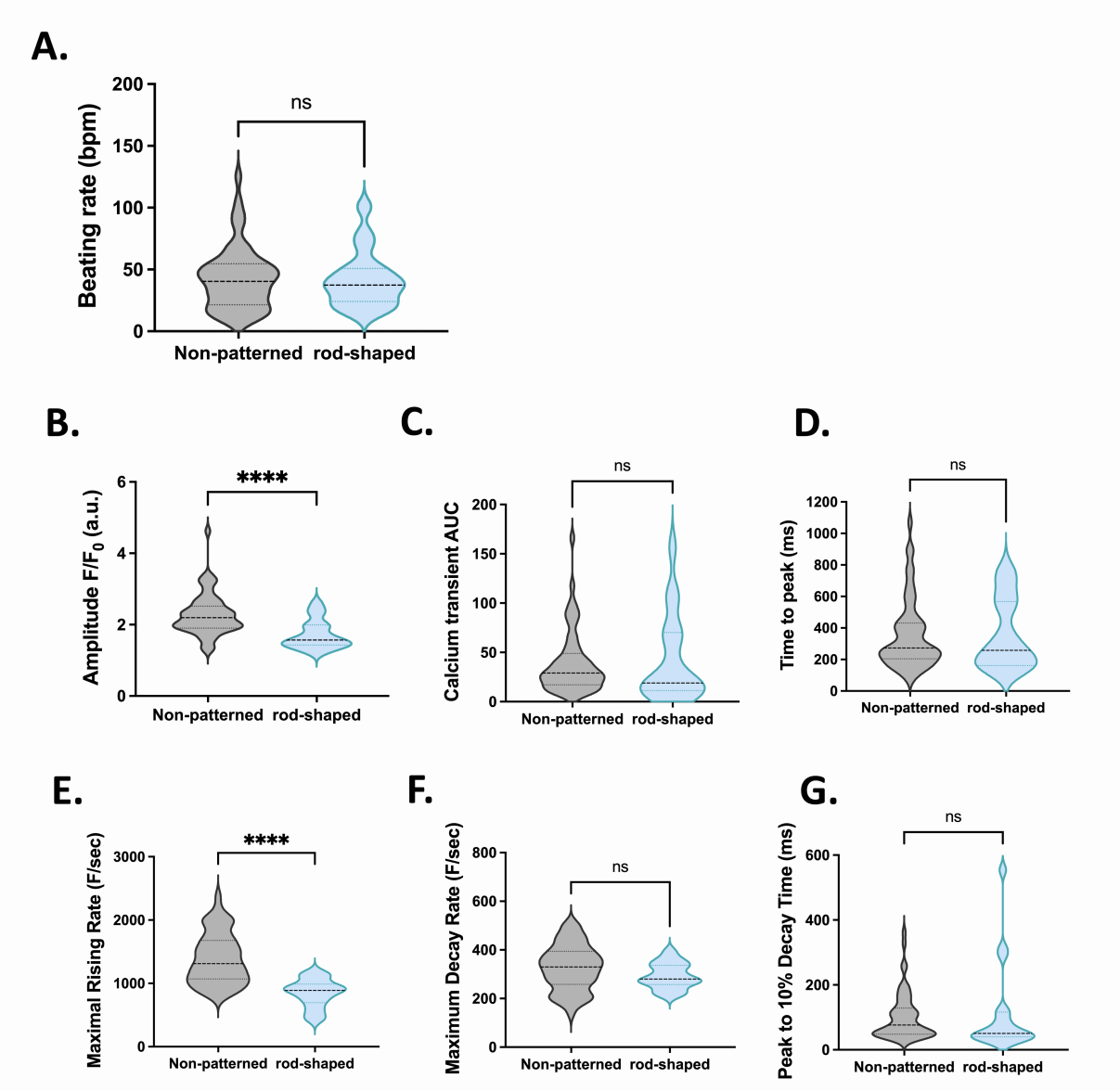

(A) Violin plot showing spontaneous beating rates from non-patterned and rod-shaped hiPSC-CMs. (B-G) Violin plots of (B) calcium transient amplitude, (C) calcium transient area under the curve, (D) time to peak, (E) maximum rising rate, (F) maximum decay rate and (G) peak to 10% decay time.
n = 18-55 cells from 3-4 independent experiments. Adjusted linear mixed effect model: ns $P>0.05$, **** $P<0.0001$ *vs.* non-patterned hiPSC-CMs

Table S1: List of primers, related to Figures 3-5, S2 and S4

Target	Forward primer	Reverse primer	Product size
RPL32	AGTTCCTGGTCCACAACGTC	GTGACTCTGATGGCCAGTTG	142
HCN4	GAACAGGAGAGGGTCAAGTCG	CATTGAAGACAATCCAGGGTGT	172
KCNJ2	GTGCGAACCAACCGCTACA	CCAGCGAATGTCCACACAC	234
KCNH2	ATGCTCATTGGCTCCCTCAT	CAGCATCTGTGTGTGGTAGC	102
SCN5a	GTCGGCATACTCAAGCAGAACC	CAAGACCTGCTACCACATCGTG	145
SERCA2a	CATCCGCTACCTCATCTCGT	AGGAATCAAAGCCTCGGGAA	88
CACNA1C	GCAGGAGTACAAGAACTGTGAGC	CGAAGTAGGTGGAGTTGACCAC	143
Adult SCN5a	CTTCACCGCCATTTACACCT	CCCAGGTCCACAAATTCAGT	150
Fetal SCN5a	CTTCACCGCCATTTACACCT	AAGAGCCGACAAATTGCCTA	166
TNNT2	CAGGATCAACGATAACCAGAAAGTC	GTGAAGGAGGCCAGGCTCTA	87
TNNI1	TCCGTGGGAAGTTCAAGCG	GACTTGGCGGCATCAAACATC	238
TNNI3	CCAACTACCGCGCTTATGC	CTCGCTCCAGCTCTTGCTTT	120
ACTN2	CAAACCTGACCGGGGAAAAAT	CTGAATAGCAAAGCGAAGGATGA	178
MYH7	GGCAAGACAGTGACCGTGAAG	CGTAGCGATCCTTGAGGTTGTA	133

Movie S1: Bright field recording of non-patterned hiPSC-CMs.

Movie S2: Bright field recording of rod-shaped hiPSC-CMs.